

LENSING IN THE HERCULES SUPERCLUSTER¹

JOHN P. BLAKESLEE^{2,3,4}, MARK R. METZGER³, HARALD KUNTSCNER², AND PATRICK CÔTÉ^{3,5,6}

To appear in AJ, January 2001

ABSTRACT

We report Keck LRIS observations of an arc-like background galaxy near the center of Abell 2152 ($z = 0.043$), one of the three clusters comprising the Hercules supercluster. The background object has a redshift $z = 0.1423$ and is situated $25''$ north of the primary component of the A2152 brightest cluster galaxy (BCG). The object is about $15''$ in total length and has a reddening-corrected R -band magnitude of $m_R = 18.55 \pm 0.03$. Its spectrum shows numerous strong emission lines, as well as absorption features. The strength of the $H\alpha$ emission would imply a star formation rate $SFR \approx 3 h^{-2} M_{\odot} \text{ yr}^{-1}$ in the absence of any lensing. However, the curved shaped of this object and its tangential orientation along the major axis of the BCG suggest lensing. We model the A2152 core mass distribution including the two BCG components and the cluster potential. We present velocity and velocity dispersion profile measurements for the two BCG components and use these to help constrain the potential. The lens modeling indicates a likely magnification factor of ~ 1.9 for the lensed galaxy, making A2152 the nearest cluster in which such significant lensing of a background source has been observed. Finally, we see evidence for a concentration of early-type galaxies at $z = 0.13$ near the centroid of the X-ray emission previously attributed to A2152. We suggest that emission from this background concentration is the cause of the offset of the X-ray center from the A2152 BCG. The background concentration and the dispersed mass of the Hercules supercluster could add further to the lensing strength of the A2152 cluster.

Subject headings: galaxies: clusters: individual (Abell 2152) — galaxies: elliptical and lenticular, cD — gravitational lensing

1. INTRODUCTION

Strong gravitational lensing of background sources by clusters of galaxies provides some of the most unambiguous evidence for the presence of large amounts of dark matter in clusters. Lensing studies suggest that the mass in clusters is greater and more centrally concentrated than implied, for instance, by the X-ray properties (e.g., Melier, Fort, & Kneib 1993; LeFèvre et al. 1994; Waxman & Miralda-Escudé 1995; Smail et al. 1995). Moreover, the mass appears to clump around the luminous galaxies, so that consideration of substructure and the effect of the massive central galaxy are often important for understanding the observations (e.g., Miralda-Escudé 1995; see also Tyson, Kochanski, & Dell Antonio 1998). This is particularly true in more moderate mass clusters with velocity dispersions $\sigma_{cl} \lesssim 1000 \text{ km s}^{-1}$, for which the proportionally larger gravitational effects of a massive cD must be included to properly account for the lensing (Williams, Navarro, & Bartelmann 1999).

Although there have been great advances in our knowledge of the form of the density distributions of massive dissipationless particles in simulations of various resolution (e.g., Dubinski & Carlberg 1991; Navarro, Frenk, & White 1996, 1997; Moore et al. 1998, 1999b), our knowledge of the central mass distributions of actual galaxy clusters remains fragmentary. Low redshift clusters, because

of their larger angular sizes, can in principle provide a better opportunity for studying these mass distributions. Their lensing properties are acutely sensitive to the shape of the inner cluster potential, although because such clusters tend to be of modest mass (very high-mass clusters being few and far between), the individual galaxies will produce relatively larger perturbations on this potential, complicating the interpretation.

Until recently, moderate- to high-redshift clusters have been the exclusive purview of strong lensing studies, but lensing by low-redshift clusters has been gaining increased attention. For instance, Allen, Fabian, & Kneib (1996) discovered a redshift $z = 0.43$ lensed arc in the massive cooling flow cluster PKS 0745–191 at $z = 0.103$. Campanano, Kneib, & Hardy (1998) explored lensing models for a $z = 0.073$ spiral galaxy located near the central elliptical in the richness class 0 cluster A3408 at $z = 0.042$; they obtained an upper limit to the magnification factor of ~ 1.7 from their “maximum mass” model. This object turned out to be the only viable lensing candidate found in an imaging survey of 33 southern galaxy clusters with $z \leq 0.076$ by Cypriano et al. (2000), who also presented an estimate of the expected number of arcs and arclets in low-redshift clusters. Blakeslee & Metzger (1999) discovered a lensed arc at $z = 0.573$ in the nearby cD cluster A2124 at $z = 0.066$ and found magnification factors near

¹Based on observations obtained at the W.M. Keck Observatory, which is jointly operated by the California Institute of Technology, the University of California, and the National Aeronautics and Space Administration.

²Department of Physics, University of Durham, South Road, Durham, DH1 3LE, United Kingdom

³California Institute of Technology, Mail Stop 105-24, Pasadena, CA 91125

⁴Current address: Department of Physics and Astronomy, Johns Hopkins University, Baltimore, MD 21218

⁵Sherman M. Fairchild Fellow

⁶Current address: Department of Physics and Astronomy, Rutgers University, 136 Frelinghuysen Road, Piscataway NJ, 08854-8019

10 from their best-fitting models of this system.

Despite the recent progress, the lensing properties of low-redshift clusters remain unclear. For instance, A2124 had by far the lowest redshift in the sample studied by Williams et al. (1999) of 24 lensing clusters with measured velocity dispersions, the next nearest being at $z = 0.171$. In this paper, we present imaging and spectroscopic observations and give a lensing analysis of the redshift $z = 0.043$ cluster Abell 2152 in the Hercules supercluster.

2. CLUSTER PROPERTIES

The Hercules supercluster is a close grouping of three Abell clusters: the richness class 2 cluster A2151 (the classical ‘‘Hercules cluster’’) and the two richness 1 clusters A2147 and A2152, all at $z \sim 0.04$. The supercluster was first identified by Shapley (1934). Although A2151 dominates from the standpoint of the number of galaxies, A2152 is projected closest to the center of the grouping, which is so tight that a circle of just 2° ($\lesssim 4 h^{-1}$ Mpc) in diameter easily encompasses all three clusters. Two other Abell clusters, A2148 and A2107, lie at about the same redshift and are only $\sim 15 h^{-1}$ Mpc away. At lower density enhancements, the Hercules supercluster forms part of an extended, filamentary supercluster that includes A2162 and A2197/A2199 about 3000 km s^{-1} in the foreground and A2052/A2063 about 3000 km s^{-1} in the background (Abell 1961; Postman, Huchra, & Geller 1992). This extended ten-cluster supercluster includes more members than any other supercluster in the Postman et al. (1992) catalogue.

All three members of the Hercules supercluster proper are classified as Bautz-Morgan type III, Rood-Sastry class F clusters (Abell et al. 1989; Struble & Rood 1987), indicating morphological irregularity and perhaps dynamical youth. All three have relatively high spiral fractions, with that of A2151 being near 50% (Tarengi et al. 1980). A2151 is also famous for its high degree of internal subclustering (e.g., Bird et al. 1995). A2152, the focus of this paper, has two bright early-type galaxies at its center (see Figure 1) that together are designated UGC 10187. The brighter component (NED 02) was chosen by Postman & Lauer (1995) as the A2152 brightest cluster galaxy (BCG) and has a redshift $z = 0.0441$. The other component (NED 01) is $47''$ to the northwest and about 0.5 mag fainter; Postman & Lauer classify it as the second ranked galaxy (SRG). The SRG has a relative velocity of $+330 \text{ km s}^{-1}$ with respect to the BCG (see §3.3).

Because A2152 and A2147 are separated by just $1.8 h^{-1}$ Mpc, measurements of their velocity dispersions are problematic. Zabludoff et al. (1993) reported $\sigma_{\text{cl}} = 1081 \text{ km s}^{-1}$ for A2147 and $\sigma_{\text{cl}} = 1346 \text{ km s}^{-1}$ for A2152, the latter being the highest dispersion in their sample of 25 ‘‘dense peaks.’’ Recently, Barmby & Huchra (1998) have carried out a detailed analysis of the Hercules supercluster kinematics using 414 galaxy velocities. These authors employed a four-component model, including the three Abell clusters and a ‘‘dispersed supercluster’’ component. They derived much lower velocity dispersions of $821_{-55}^{+68} \text{ km s}^{-1}$ and $715_{-61}^{+81} \text{ km s}^{-1}$ for A2147 and A2152, respectively, from 93 and 56 galaxy velocities.

Because 122 galaxies in the Barmby & Huchra sample are assigned to the dispersed component with a high velocity dispersion of 1407 km s^{-1} , rather than to one of

the individual clusters, this approach may tend to bias the cluster dispersions low. However, it is clearly more consistent in finding a mean redshift of $\langle z \rangle = 0.0432$ for A2152, much closer to that of the BCG, whereas previous studies found means 10–15% lower, near the mean values for A2147 and A2151. Moreover, the lower velocity dispersions are more in line with the X-ray properties of these clusters, e.g., the X-ray gas temperature in A2152 has been estimated from *Einstein* data to be $kT_X = 2.1 \text{ keV}$ (White, Jones, & Forman 1997). We note, however, that the latest tabulation by Struble & Rood (1999) lists $\langle z \rangle = 0.0398$ and $\sigma_{\text{cl}} = 1338 \text{ km s}^{-1}$ for A2152 from 62 velocities.

The centroid of the X-ray emission associated with A2152 is not coincident the BCG but is about 2'.1 east. Its position is within $40''$ of a pair of bright early-type galaxies which the Barmby & Huchra redshift catalogue reveals to be at $z = 0.134$. Each of these background galaxies is intrinsically $\sim 70\%$ more luminous than the A2152 BCG (using a relative K-correction of 0.11 mag for ellipticals). We return to this point in §5.

3. OBSERVATIONS

A2152 was observed as part of the deep *R*-band Keck imaging study by Blakeslee (1999) of the BCG halo regions in six nearby rich clusters. Clusters were selected to have velocity dispersions similar to that of the Coma cluster and to lie in the redshift range $cz = 10,000\text{--}20,000 \text{ km s}^{-1}$. These six were then observed because they were reachable during a single night in the northern spring. Based on this dataset, Blakeslee & Metzger (1999) reported follow-up spectroscopy of a magnitude $m_R = 20.86$ lensed arc located $27''$ from the center of the cD galaxy in Abell 2124. We have visually searched the dataset for other bright lensing candidates, based on proximity to the BCG, tangential orientation, and arc-like appearance. The only obvious bright candidate was an arc-like object in A2152. We obtained follow-up Keck spectroscopy for this object and the A2152 BCG/SRG pair.

3.1. Imaging Data

The imaging observations have already been described in detail by Blakeslee (1999). Here we summarize them and report new photometric results for the A2152 arclet. A2152 was imaged with the Low Resolution Imaging Spectrograph (LRIS, Oke et al. 1995) on the Keck II telescope under photometric conditions. The image scale was $0''.211 \text{ pix}^{-1}$, and the total integration was 2000 s in the *R* band. Reductions were carried out using the Vista package. The seeing in the final stacked image was an exceptional $0''.53$. The photometry was calibrated to the Cousins *R* band using Landolt (1992) standard stars; the photometric zero point is accurate to better than 0.02 mag.

Figure 1 displays the A2152 Keck LRIS image, a smaller portion of which was shown by Blakeslee (1999). The possible lensed galaxy (galaxy ‘‘A’’) is located $25''.2$ from the center of the BCG at a position angle $\text{PA} = 11^\circ.4$. The major axis of the BCG is at $11^\circ \pm 2^\circ$ at radii $\lesssim 15''$, where the ellipticity (difference of the axis ratio from unity) of the light distribution is $\epsilon_\ell = 0.10$. Beyond this radius the BCG isophotes have significant overlap with those of the SRG and they are sufficiently round that the angle is difficult to determine. The isophotes of the SRG show significant twisting; the PA of its major axis swings from 170° at

$r \lesssim 5''$ to $\sim 136^\circ$ by $r \approx 25''$, while the ellipticity stays fairly constant around $\epsilon_\ell = 0.32 \pm 0.03$.

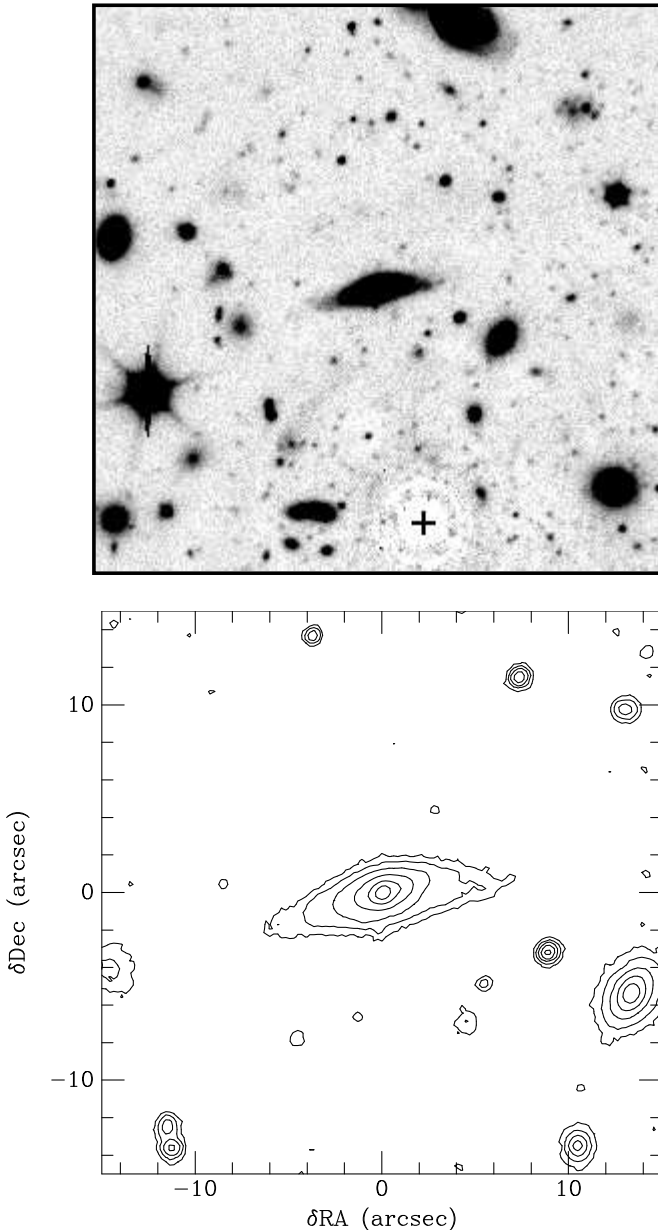


FIG. 2.— Two views of the possibly lensed galaxy in A2152 (galaxy A). North is up and east is to the left. The top view shows a $1' \times 1'$ region of the R -band LRIS image centered on the galaxy. The stretch is linear, and a model of the BCG/SRG halo light has been subtracted. The cross marks the center of the subtracted BCG, which is $25''$ from A. The lower panel zooms in by a factor of two, showing an isophotal contour map of the $30''$ square region around A. The outermost contour is at an extinction-corrected surface brightness of $24.8 \text{ mag arcsec}^{-2}$, corresponding 2.0% of the sky level in the image, and the other contours are in steps of 1 mag. The curvature of the object is apparent in both panels.

All galaxies with known redshifts (either from Barmby & Huchra or the present study) are labeled in Figure 1. It is somewhat curious that of 7 galaxies (including galaxy A) in the central $\sim 6'$ field of a rich cluster, only 3 turn out to be cluster members. As mentioned above, the galaxy pair

G1/G2 are in the background with redshifts of $z = 0.1335$ and $z = 0.1353$, respectively. During our spectroscopic observation of the BCG/SRG (described in §3.3), the LRIS slit picked up the magnitude $m_R = 19.2$ galaxy labeled G3, which turns out to have $z = 0.1326$. Galaxy “M” is an A2152 member with a velocity within $\sim 100 \text{ km s}^{-1}$ of the BCG (Barmby & Huchra). The center of the X-ray emission in this field (Jones & Forman 1999) is $20''$ from G2 and $50''$ from G1 and is also labeled in Figure 1.

Figure 2 shows an enlarged view of galaxy A along with an isophotal contour map. The impression is that of a disk galaxy whose disk has been warped into an arc-like shape (arguably through lensing, as we discuss in §4). The object is visible in our image for a length of about $15''$. The measured full-width at half maximum along the minor axis is $0''.67$, which would be about $\text{FWHM} \sim 0''.4$ in the absence of atmospheric blurring. This translates to a metric size $\lesssim 0.7 h^{-1} \text{ kpc}$ at the redshift of this object (see below); apparently it has a very compact nucleus. The total magnitude of A, corrected for 0.105 mag of R -band Galactic extinction (Schlegel, Finkbeiner, & Davis 1998), is $m_R(\text{arc}) = 18.55 \pm 0.03$. Our main measurement results are collected in Table 1.

3.2. Spectroscopy of Galaxy A

The simplest and most important test of gravitational lensing is whether or not the supposed lensed object is actually in the background. Thus, we obtained one 900 s spectrum of galaxy A with LRIS on the Keck II telescope on the night of 25 March 1999 (UT). We used a 300 line grating and a $1''$ wide slit oriented at $\text{PA} = 113^\circ$, approximately along the major axis of galaxy A. The seeing was poor, about $1''.8$, so the slit missed a good fraction of the light. The dispersion was $2.44 \text{ \AA pix}^{-1}$, and the effective resolution was about 10 \AA (FWHM). Halogen flats and arc-lamp exposures were taken for calibration. The LRIS configuration and IRAF reductions were identical to those of Blakeslee & Metzger (1999), except that no flux standard spectrum was obtained.

Figure 3 shows the reduced 1-d spectrum of galaxy A with the strongest emission lines labeled at top and some absorption lines labeled at the bottom. The emission appeared to be confined to the central $\sim 4''$ of the galaxy, so this is all that was extracted. The spectrum is of very high signal-to-noise (it was not a priori obvious, in the absence of spiral structure or any spectral information, that there would be such strong features), and we determine the redshift to be $z = 0.1423 \pm 0.0001$. The object is therefore about 3.3 times more distant than the intervening A2152 cluster, and the lensing hypothesis remains viable. If unlensed, the absolute magnitude of A, with a K-correction of 0.05 mag, would be $M_R = -20.57$ (for $h = 0.7$ and $\Omega = 0$; $M_R = -21.22$ for $h = 0.5$ and $\Omega = 1$), or a luminosity of about $0.48 L_R^*$ (e.g., Lin et al. 1996).

The $\text{H}\alpha$ emission line has an equivalent width of $\text{EW}_{\text{H}\alpha} = 117 \pm 6 \text{ \AA}$, corrected for $[\text{N II}]$ emission. The $\text{H}\beta$ equivalent width is $\text{EW}_{\text{H}\beta} = 28.2 \pm 2.0 \text{ \AA}$. The $[\text{O II}] \lambda 3727$ and $[\text{O III}] \lambda 5007$ lines have equivalent widths of $83.3 \pm 2.3 \text{ \AA}$ and $54.1 \pm 2.0 \text{ \AA}$, respectively. Thus, the emission is quite strong, but not too anomalous in comparison to many late-type spirals or irregulars (e.g., Kennicutt 1992).

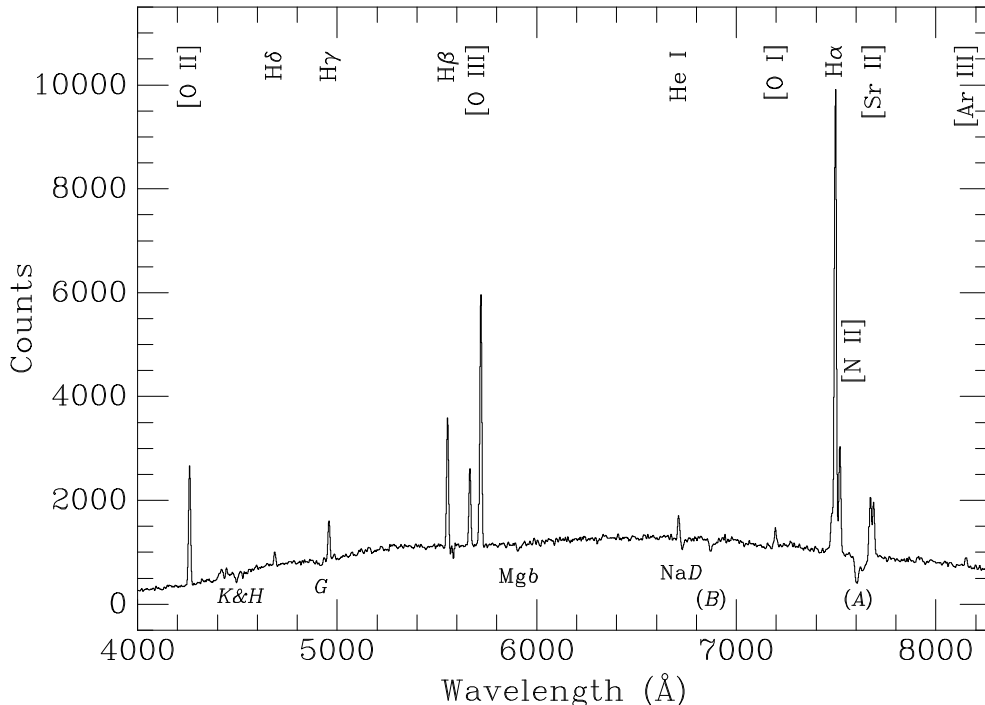


FIG. 3.— Reduced 1-d spectrum of galaxy A. The redshift is $z = 0.1423$. Various emission lines are identified above the spectrum and some absorption features are labeled at bottom, including the Ca II H and K lines, G band, $Mg b$, and $Na D$. The atmospheric A and B absorption bands are also labeled; A -band absorption affects the [Sr II] lines, but not $H\alpha$.

Although we do not have a good absolute flux calibration of the spectrum, we can roughly estimate the star formation rate (SFR) from the $H\alpha$ equivalent width and the R -band luminosity. We use the spectrophotometric synthesis results of Fukugita, Shimasaku, & Ichikawa (1995) to calibrate the absolute flux in Cousins R , which has an effective wavelength of 6588 \AA . About 75% of the R -band light comes from the region of emission within the galaxy, and from the measured $H\alpha$ equivalent width we obtain a flux $f_{H\alpha} \approx 7.38 \times 10^{-15} \text{ ergs s}^{-1} \text{ cm}^{-2}$ and a luminosity of $L_{H\alpha} \approx 1.84 \times 10^{41} \text{ h}^{-2} \text{ ergs s}^{-1}$ ($\Omega = 0$). To estimate the internal extinction, we perform a makeshift relative flux calibration using the Feige 110 spectrum from Blakeslee & Metzger (1999) and find an $H\alpha$ -to- $H\beta$ flux ratio of 4.25; assuming an unextincted value of 3.0 and the extinction curve of Cardelli, Clayton & Mathis (1989) gives a correction at $H\alpha$ of a factor of 2.15. This is close to the “canonical” correction of ~ 1 mag for spirals (e.g., Kennicutt 1992) but will yield a SFR 16% lower. Finally, using the updated calibration from Kennicutt (1998), we find $\text{SFR} \approx (3 \pm 1) \text{ h}^{-2} \text{ M}_{\odot} \text{ yr}^{-1}$, or $(6 \pm 2) \text{ M}_{\odot} \text{ yr}^{-1}$ for a typical H_0 . Though not qualifying as a “starburst galaxy,” the SFR is quite substantial for a $0.5 L^*$ galaxy. The quoted errorbar is approximate and reflects mainly the $\sim 30\%$ scatter quoted by Kennicutt. The calibration based on [O II] equivalent width yields nearly the same SFR for this galaxy.

3.3. Kinematics of the Central Galaxy

With the intent of improving the constraints on the A2152 potential for the lensing models, we obtained three 1100 s spectra of the BCG/SRG pair with LRIS on 16 June

1999. We again used a $1''$ wide slit but the 900/5500 grating, yielding a dispersion of $0.84 \text{ \AA pix}^{-1}$. The slit was oriented at $\text{PA} = 122^\circ$ in order to pass through the centers of the two galaxies. Again, halogen flats and arc lamps were taken for calibration, and we also obtained spectra of the K4 III velocity standard HD 213947. The spectra were processed, wavelength calibrated, and rectified using standard IRAF routines.

Figure 4 displays the central $1'' \times 1''$ extracted from the reduced 2-d spectra. Although the spectra are clearly very similar, the BCG exhibits a small amount of $H\beta$ emission that is absent from the SRG. Such optical line emission is quite common among central cluster galaxies, and may be associated with cluster “cooling flows” (e.g., Crawford et al. 1999). This emission may therefore be evidence that the BCG is indeed at the center of the A2152 cluster potential and that the offset of the Jones & Forman (1999) X-ray position is due to contamination from a background X-ray source.

The kinematical analysis of the data was performed within the MIDAS package. First, the spectra were rebinned along the slit (spatial direction) in order to achieve a minimum signal-to-noise (S/N) of 30 per \AA at all radii. The S/N of the central pixels is higher. Then the continuum was removed by a fifth order polynomial fit. Finally we determined the velocity dispersion and rotational velocity as a function of radius with the Fourier Correlation Quotient (FCQ) method (Bender 1990) allowing only for a Gaussian stellar velocity distribution. When we allowed for non-Gaussian distributions and fitted for the higher-order moments, the results for the rotational velocity and

dispersion were unchanged within the errors but showed slightly more scatter at the largest radii. The detailed FCQ setup, such as continuum fit order, wavelength extraction and error estimation was optimized with Monte Carlo simulations.

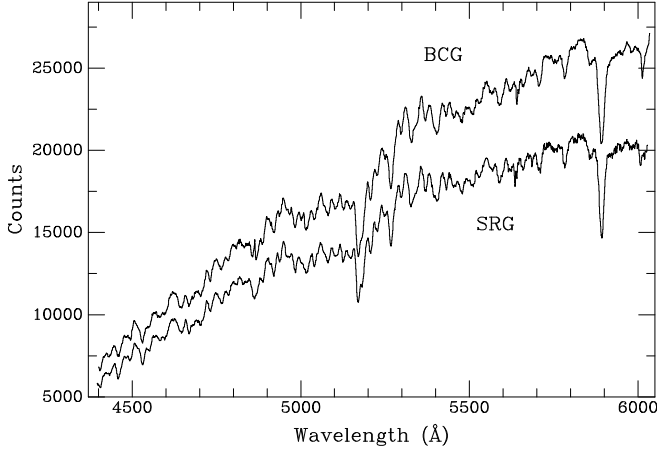


FIG. 4.— The central $1''.1$ extracted from the 2-d spectra of the BCG and SRG (observed simultaneously through the slit) are illustrated. The spectra have been deredshifted for purposes of comparison. Some emission is visible within the $H\beta$ absorption at $\lambda = 4861 \text{ \AA}$ in the spectrum of the BCG, but not in the SRG.

Figure 5 shows the measured velocity and velocity dispersion profiles for the BCG and SRG. Note that the 122° position angle is $\sim 70^\circ$ away from the major axis of the BCG, and so the profile is more appropriate to the minor axis. For the SRG, the PA is closer to the major axis. Both galaxies show significant rotation, and both rotate in the sense opposite to that of the combined BCG/SRG system. Although the velocity dispersions decline outward from the centers of the galaxies, the dispersion profile for the SRG appears to flatten at a value of $\sigma \sim 230 \text{ km s}^{-1}$ outside the central $3''$. Likewise, the BCG’s velocity dispersion profile does not show a significant decrease for $r \gtrsim 7''$. As seen in the top panel of Figure 5, the center of rotation in the BCG is offset by about $0''.2$ (1 LRIS pixel) from the luminosity center; this is likely due to a slight offset of the galaxy center within the slit. The mean velocities, rotational velocities, and central dispersions are tabulated along with our other results in Table 1.

We have estimated the total (1-sigma) errors on the mean velocities to be $\pm 25 \text{ km s}^{-1}$, but this is dominated by zero-point calibration errors (flexure, illumination of slit, etc.). However, the relative velocity of the BCG/SRG pair is better determined at $\Delta v = 331 \pm 7 \text{ km s}^{-1}$. This accords well with previous measurements of $\Delta v = 327 \pm 100 \text{ km s}^{-1}$ from Tarenghi et al. (1979) and $\Delta v = 341 \pm 50 \text{ km s}^{-1}$ from Wegner et al. (1999); less well with $\Delta v = 502 \pm 21 \text{ km s}^{-1}$ from Davoust & Considère (1995). (The velocities used by Barmby & Huchra for these two galaxies come from Tarenghi et al.).

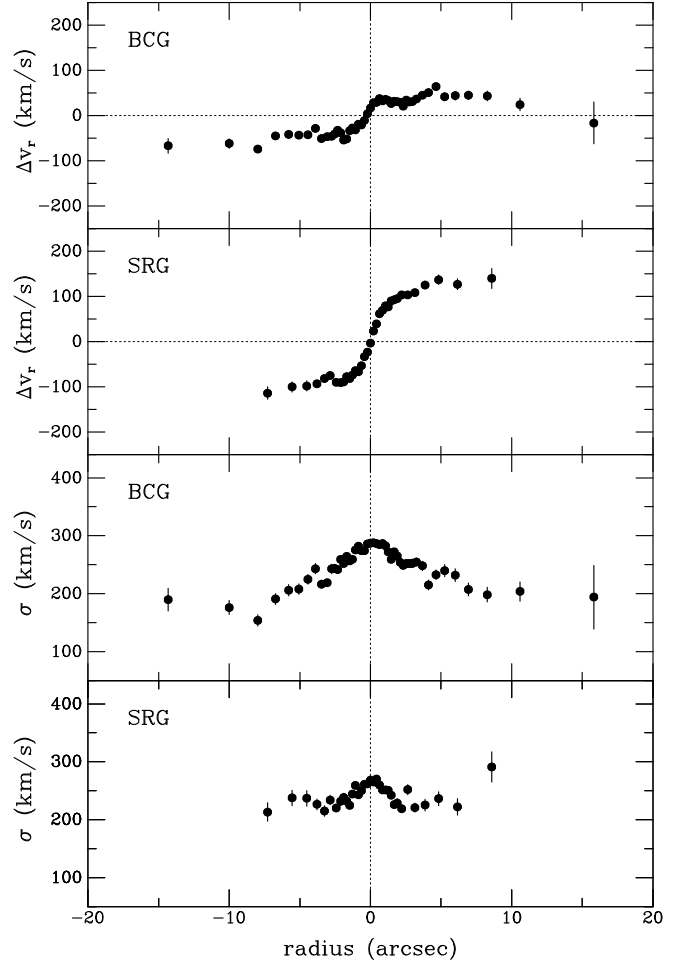


FIG. 5.— Velocity and dispersion profiles for the BCG and SRG (labeled). Note that the radial coordinate defined here increases to the southeast along the slit, i.e., the BCG is in the direction of positive radius with respect to the SRG. Thus, the point in the SRG’s dispersion profile at $(r, \sigma) = (8''.6, 291)$ may be beginning to show the effects of the BCG halo light.

Central velocity dispersions have been measured previously for the BCG by Oegerle & Hoessel (1991), who found $\sigma_0 = 295 \pm 25 \text{ km s}^{-1}$, and by Wegner et al. (1999), who reported $\sigma_0 = 280 \pm 26 \text{ km s}^{-1}$; both results are in agreement with our much more precise value of $\sigma_0 = 295 \pm 7 \text{ km s}^{-1}$. For the SRG, we find a central dispersion of $\sigma_0 = 271 \pm 8 \text{ km s}^{-1}$, while Wegner et al. found $\sigma_0 = 313 \pm 34 \text{ km s}^{-1}$. Their significantly higher dispersion is likely due to the strong rotation in this galaxy, which these authors did not account for when extracting the spectrum of the central several arcseconds of the galaxy. Finally, our BCG mean velocity is $\sim 2.5 \sigma$ discrepant with the Wegner et al. value, which is higher by 95 km s^{-1} , but it agrees within the errors with the values from Tarenghi et al. (1979), Oegerle & Hoessel (1991), and Davoust & Considère (1995). No previous measurements of the rotation or dispersion profile in either galaxy could be found.

Finally, as noted in §3.1, the LRIS slit picked up the magnitude $m_R = 19.24$ galaxy labeled G3 in Figure 1. We find it to be in the background with a velocity $cz = 39,738 \text{ km s}^{-1}$. This is just $\sim 290 \text{ km s}^{-1}$ less than the velocity of G1 and $\sim 830 \text{ km s}^{-1}$ less than that of G2.

4. IS IT LENSED?

To model A2152 as a lens, we use a potential of the form (Blandford & Kochanek 1987)

$$\psi(r') = 4\pi \left(\frac{\sigma_{1D}}{c}\right)^2 \frac{D_{LS}}{D_S} \left[\left(1 + \frac{r'^2}{r_c^2}\right)^{\frac{1}{2}} - 1 \right],$$

where σ_{1D} is the line-of-sight velocity dispersion in the limit $r' \gg r_c$ for the spherical case, D_S and D_{LS} are angular size distances to the source and from the lens to the source, respectively, and r_c defines a softening radius. An ellipticity parameter ϵ_p can be introduced through $r'^2 = (1-\epsilon_p)x^2 + (1+\epsilon_p)y^2$, where (x, y) are coordinates aligned with the major and minor axes of the potential. This represents a softened isothermal sphere for $\epsilon_p = 0$ and provides a fairly good representation of the dark halo potentials in the cores of clusters (e.g., Mellier et al. 1993; Tyson et al. 1998). We use the more limited relation with a fixed power law because there are too few lensing constraints in this system to differentiate various potential profiles, and we have used only circularly symmetric potentials as there is little constraint on the ellipticity.

We explored four different simple models for the lensing potential. We included three terms in each of these models, corresponding to the smooth halo mass in the cluster and the masses associated with the BCG and SRG. For the latter two components, we use analytic potentials to approximate the velocity dispersions measured in §3.3 with a small core. In our model 1, the center of the cluster potential was fixed at the cD center with an asymptotic dispersion of $\sigma_{cl} = 715 \text{ km s}^{-1}$ as measured by Barmby & Huchra (1998) and a softened core radius of $10''$. Model 2 also fixes the cluster potential at the BCG, but uses the higher dispersion estimate of 1340 km s^{-1} (Struble & Rood 1999). Models 3 and 4 are the same as models 1 and 2, but fix the cluster potential center at the X-ray center (while of course keeping the BCG and SRG model components fixed). Within each model, we also explored a range of core softening radii.

Our primary constraints for the lens models are the radius, size, and orientation of galaxy A. The modest distortion and lack of a counterarc suggests a source position that lies outside the tangential and radial caustics (e.g., Grossman & Narayan 1988) and whose image lies outside the critical curve. These constraints quickly rule out model 2 in most forms: with a small core radius, the critical curve for $z = 0.142$ lies at around 35 arcsec, well outside the galaxy radius. This would imply multiple images and large distortions for galaxy A. Even with a large core radius, the effective radial magnification becomes large and can be ruled out by the lens appearance. Model 3 does not produce significant magnification or distortion for the galaxy; thus under such a model, the arc-like shape would need to be intrinsic. Model 4 produces shear and magnification at the position of galaxy A, but the shear direction is not directed tangential to the BCG, as observed in galaxy A.

Model 1, however, produces modest magnification and distortion of a $z = 0.142$ source with a shear aligned tangentially to the BCG/cluster. A family of models with a range of core radii and asymptotic dispersions for the pri-

mary lens (cluster dark matter) can reproduce the characteristics of the arc. These models are degenerate in σ_{1D} and r_c for determining the mass enclosed within the arc radius. Model 1 fits within this family of models. Figure 6 shows the predicted magnifications from model 1 with a $10''$ core as a function of observed source position. The position of galaxy A implies a magnification of ~ 1.9 , dropping to ~ 1.8 for a model with a $40''$ soft core. Given this model, we can ask what the intrinsic source shape of galaxy A would be; Figure 7 shows contours of the observed galaxy surface brightness along with the same contours mapped back to the source plane via the lens equation. The implied shape is that of a fairly symmetric galaxy with a disk and dominant bulge, with no indication of a warp.

While we cannot make quantitative estimates of cluster mass parameters with a single lensed galaxy, we find that a simple model constructed from a low-dispersion cluster centered at the BCG can produce the shear needed to explain the curved shape of the background galaxy from a more symmetric source. Indeed, galaxy A must be distorted in some fashion by the foreground cluster, and we can rule out two of our other three plausible models based on the implied lensing geometry. We cannot, however, rule out a low-dispersion cluster mass centered on the X-ray center from lensing alone, although this would mean galaxy A must be intrinsically warped. Another galaxy with an unusual shape, elongated *radially* from the BCG center, is visible about $11''$ to the east of the BCG (see the upper panel of Fig. 2) and lies near some critical radii of model 1. If in the background, this galaxy may provide much better constraints on the shape of the inner potential, however the redshift is unknown and we do not attempt to model it here.

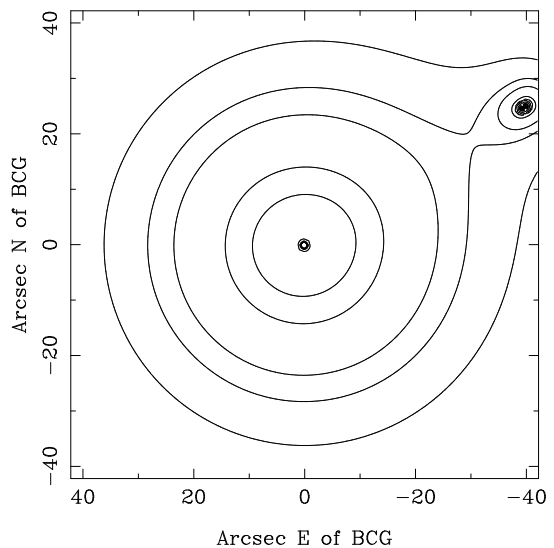


FIG. 6.— Magnification of a background source at $z = 0.142$ produced by the simple lens model. The model shown has $\sigma_{cl} = 715 \text{ km s}^{-1}$ with a 10 arcsec soft core, $\sigma_{BCG} = 250 \text{ km s}^{-1}$, and $\sigma_{SRG} = 240 \text{ km s}^{-1}$. Starting from the outside, contours indicate magnifications of 1.5, 1.73, 2, 4, and 16. The critical curve is near the magnification=16 contour, and a second critical curve is present close to the center.

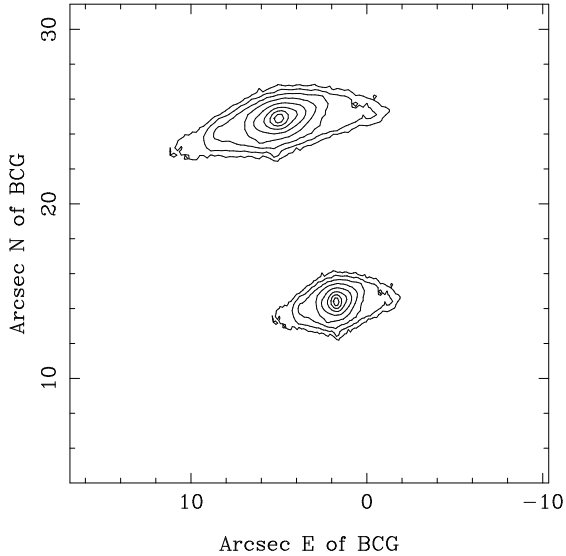


FIG. 7.— Contours of the observed galaxy and the inferred source contours from the simple lens model. The upper image shows contours of the observed surface brightness of the lensed galaxy A, spaced by factors of two. The lower image shows the implied source position and the same surface brightness contours on the source plane, i.e. how the galaxy would appear if the foreground cluster were absent. The innermost contours, less than $1''$ in size, are rounded in the observed image from the seeing; therefore, these contours become artificially elongated in the reconstructed source image. The coordinates are centered on the BCG.

5. SUMMARY AND DISCUSSION

Deep R -band Keck imaging taken under excellent seeing conditions has revealed a curved object $25''.2$ ($15 h^{-1}$ kpc) from the center of the A2152 BCG, along the major axis. The reddening-corrected R magnitude of this “arc” is $m_R = 18.55 \pm 0.03$, and follow-up spectroscopy shows that it lies at a redshift $z = 0.1423 \pm 0.0001$. Its position, orientation, and redshift all suggest a lensing explanation for the curiously bowed structure. The object has numerous strong emission lines, and the equivalent width of $H\alpha$ is $117 \pm 6 \text{ \AA}$, from which we infer a star formation rate of $(3 \pm 1) h^{-2} M_{\odot} \text{ yr}^{-1}$.

We have presented spatially resolved spectroscopy of the A2152 BCG and SRG, which are separated by $47''$ and are together catalogued as UGC 10187. The relative velocity of the BCG and SRG is $331 \pm 7 \text{ km s}^{-1}$, and both galaxies show significant rotation. The rotational velocities along the observed position angle are $\sim 50 \text{ km s}^{-1}$ and $\sim 120 \text{ km s}^{-1}$ for the BCG and SRG, respectively. Our velocity dispersion profile for the BCG extends to a radius of $\sim 16''$ ($9.5 h^{-1}$ Mpc), about 60% of the way to the radial position of the lensed galaxy.

We have modeled the lensing potential of A2152 using constraints from the measured cluster velocity dispersion of 715 km s^{-1} and our own stellar velocity dispersion measurements for the BCG and SRG. The models cannot produce a significant lensing effect on galaxy A if the A2152

potential center is taken to coincide with the peak of the overall X-ray emission. However, if the potential center is taken to be the A2152 BCG, then the models *can* reproduce the observed position and apparent bowed shape of the galaxy, and the implied magnification is a factor of about 1.9. Conversely, we can say that if the object is significantly lensed, then the $2'1$ offset of the X-ray centroid from the BCG is due to contamination from another source of X-ray emission. We note that both the cluster velocity dispersion and the core softening radius in our lensing model is degenerate with the source position. However, the higher values that have been reported for the dispersion (see §2), if centered on the BCG, produce lens models with critical curves that lie outside of the lensed galaxy, thus multiple images would be expected of any background galaxy at the position and redshift of A. We can therefore rule out this case from a lensing argument; even a large core radius model would produce significantly more distortion in a $z = 0.142$ galaxy.

The available redshift data provide evidence for a background association of early-type galaxies at $z \approx 0.134$, projected near the center of A2152. Two of the galaxies, which we call G1/G2, have redshifts from the Barmby & Huchra (1998) catalogue. They are separated by $30''$ and are each about 70% more luminous than the A2152 BCG. The third galaxy, called G3, is $35''$ southeast of the A2152 BCG and was picked up by the LRIS slit during our observations. It is $116''$ from G1 and $132''$ from G2, or metric distances of $188\text{--}215 h^{-1}$ kpc. The velocity range for these three galaxies is $\sim 830 \text{ km s}^{-1}$. While three galaxies do not a cluster make, the luminosities, velocities, and early-type morphologies of the galaxies are highly suggestive. Moreover, there is a strong concentration of small galaxies of unknown redshift centered near the bright G1/G2 pair. It is highly likely that some of the X-ray emission, which is centered just $20''$ from G2, could be due to a grouping of galaxies associated with G1/G2. Therefore, the center of the true A2152 X-ray emission, and the center of the A2152 cluster potential, might well coincide with the A2152 BCG, as required by our lensing models. We note that the centers of the outermost X-ray contours in the Jones & Forman map of this field drift away from G1/G2 and closer to the A2152 BCG; the optical $H\beta$ emission we find in the BCG spectrum may be additional circumstantial evidence for central location in the cluster potential. However, a high-resolution X-ray map is needed to confirm this hypothesis.

If there is a background cluster, galaxy A may well be a member, in which case it would be falling away from us through the cluster with a velocity of $\sim 2500 \text{ km s}^{-1}$. Simulations show that the tidal effects of clusters on infalling galaxies can warp spiral disks into arc-like shapes (Moore et al. 1999a) and even form giant arcs of tidal debris (Calcáneo-Roldán et al. 2000). Thus, tidal interaction with a local cluster potential, rather than lensing by the foreground A2152 potential, could be responsible for the distorted appearance of the galaxy, as well as for the observed strong star formation. Its location and orientation with respect to the A2152 BCG would then be merely fortuitous. However, the galaxy in question would have to be caught during its initial pass through the cluster, since gas in cluster galaxies tends to be lost on relatively short time-scales, truncating the star formation (e.g., Balogh

et al. 1998; Kodama & Bower 2000). The probability that galaxy A is a member of a cluster at $z = 0.13$ depends of course on the velocity dispersion of the cluster. A deep redshift survey of this field is needed to discern whether or not there is a very substantial background cluster (as suggested by the luminosities of G1/G2 and the position of the X-ray center in this field), and how likely galaxy A's membership is. Such a redshift survey would need to go at least ~ 2 mag fainter than the Barmby & Huchra (1998) limit in order to pick up the multitude of small galaxies that lie between the A2152 BCG/SRG pair and the G1/G2 background pair.

Although superficially A2152 might have seemed an unremarkable low-redshift cluster (leaving aside the unlikely velocity dispersions in excess 1300 km s^{-1} found in the literature), our photometric and spectroscopic observations of its central field have raised a host of intriguing new questions about this cluster and the arc-shaped galaxy projected near its BCG. How much mass is there along this line of sight and how is it distributed? Is the A2152 BCG actually at the center of the cluster potential and the observed offset with respect to the X-ray center due to the superposed emission of a background cluster at $z = 0.13$? If so, is the distorted galaxy a member which is being distorted by the hypothetical background cluster, or is it a field galaxy being lensed by A2152? Along with high-resolution X-ray observations and a deep redshift survey, a weak lensing analysis of this field would help in unraveling the projected mass distribution and provide insight into

these questions.

We believe that the weight of the evidence favors the view that the A2152 BCG is at the center of its cluster's potential and is significantly lensing galaxy A. Further lensed objects, if present near critical curves, could provide useful future constraints on the central structure of rich clusters. For now, however, a complete understanding of this system and definitive answers to the questions raised by this study must await an infusion of new data.

We thank Michael Balogh, Alastair Edge, Ben Moore, Ian Smail, and Graham Smith for helpful conversations. This work made use of the NASA/IPAC Extragalactic Database (NED), operated by the Jet Propulsion Laboratory at Caltech under contract with the National Aeronautics and Space Administration. It also made use of Starlink computer facilities. We are grateful to the team of scientists and engineers responsible for producing the Low Resolution Imaging Spectrograph. J.P.B. and P.C. thank the Sherman Fairchild Foundation for support while at Caltech. M.R.M.'s research was supported by Caltech. J.P.B. and H.K. were supported at the University of Durham by a PPARC rolling grant in Extragalactic Astronomy and Cosmology.

Note added in proof—*New multi-color data confirm the presence of a rich background cluster around the $z = 0.13$ G1/G2 galaxy pair; analysis of these data will be presented in a forthcoming paper.*

REFERENCES

- Abell, G. O. 1961, *AJ*, 66, 607
 Abell, G. O., Corwin H. G. & Olowin, R. P. 1989, *ApJS*, 70, 1
 Allen, S. W., Fabian, A. C. and Kneib, J. P. 1996, *MNRAS*, 279, 615
 Balogh, M. L., Schade, D., Morris, S. L., Yee, H. K. C., Carlberg, R. G. & Ellingson, E. 1998, *ApJ*, 504, L75
 Barmby, P. & Huchra, J. P. 1998, *ApJ*, 115, 6
 Bender, R. 1990, *A&A*, 229, 441
 Bird, C. M., Davis, D. S., & Beers, T. C. 1995, *AJ*, 109, 920
 Blakeslee, J. P. 1999, *AJ*, 118, 1506
 Blakeslee, J. P. & Metzger, M. R. 1999, *ApJ*, 513, 592
 Blandford, R. D. & Kochanek, C. S. 1987, *ApJ*, 321, 658
 Calcáneo-Roldán, C., Moore, B., Bland-Hawthorn, J., Malin, D. & Sadler, E. M. 2000, *MNRAS*, 314, 324
 Campusano, L. D., Kneib, J.-P., & Hardy, E. 1998, *ApJ*, 496, L79
 Cardelli, J. A., Clayton, G. C. & Mathis, J. S. 1989, *ApJ*, 345, 245
 Crawford, C. S., Allen, S. W., Ebeling, H., Edge, A. C. & Fabian, A. C. 1999, *MNRAS*, 306, 857
 Cypriano, E. S., Sodr e, L., Campusano, L. E., Kneib, J.-P., Giovanelli, R., Haynes, M. P., Dale, D. A., & Hardy, E. 2000, *AJ*, submitted (astro-ph/0005200)
 Davoust, E. & Consid re, S. 1995, *A&AS*, 110, 19
 Dubinski, J. and Carlberg, R. G. 1991, *ApJ*, 378, 496
 Fukugita, M., Shimasaku, K., & Ichikawa T. 1995, *PASP*, 107, 945
 Grossman, S. A. & Narayan R. 1988, *ApJ*, 324, L37
 Jones, C. & Forman, W. 1999, *ApJ*, 511, 65
 Kennicutt, R. C. 1992, *ApJ*, 388, 310
 Kennicutt, R. C. 1998, *ARA&A*, 36, 189
 Kodama, T. & Bower, R. G. 2000, *MNRAS*, submitted (astro-ph/0005397)
 Landolt, A. U. 1992, *AJ*, 104, 340
 LeF vre, O., Hammer, F., Angonin, M. C., Gioia, I. M., & Luppino, G. A. 1994, *ApJ*, 422, L5
 Lin, H., Kirshner, R. P., Sheckman, S. A., Landy, S. D., Oemler, A., Tucker, D. L., & Schechter, P. L., 1996, *ApJ*, 464, 60
 Mellier, Y., Fort, B., & Kneib, J.-P. 1993, *ApJ*, 407, 33
 Miralda-Escud e, J. 1995, *ApJ*, 438, 514
 Moore, B., Governato, F., Quinn, T., Stadel, J. & Lake, G. 1998, *ApJ*, 499, L5
 Moore, B., Lake, G., Quinn, T. & Stadel, J. 1999a, *MNRAS*, 304, 465
 Moore, B., Quinn, T., Governato, F., Stadel, J. & Lake, G. 1999b, *MNRAS*, 310, 1147
 Navarro, J. F., Frenk, C. S., & White, S. D. M. 1996, *ApJ*, 462, 563
 Navarro, J. F., Frenk, C. S. and White, S. D. M. 1997, *ApJ*, 490, 493
 Oegerle, W. R. & Hoessel, J. G. 1991, *ApJ*, 375, 15
 Oke, J. B., Cohen, J. G., Carr, M., Cromer, J., Dingizian, A., Harris, F. H., Labrecque, S., Lucinio, R., Schaal, W., Epps, H., & Miller, J. 1995, *PASP*, 107, 307
 Postman, M. Huchra, J. P., & Geller, M. J. 1992, *ApJ*, 384, 404
 Postman, M. & Lauer, T. R. 1995, *ApJ*, 440, 28
 Schlegel, D., Finkbeiner, D., & Davis, M. 1998, *ApJ*, 500, 525
 Shapley, H. 1934, *MNRAS*, 94, 53
 Smail, I., Hogg, D. W., Blandford, R., Cohen, J. G., Edge, A. C., & Djorgovski, S. G. 1995, *MNRAS*, 277, 1
 Struble, M. F. & Rood, H. J. 1987, *ApJS*, 63, 555
 Struble, M. F. & Rood, H. J. 1999, *ApJS*, 125, 35
 Tarengi, M., Chincarini, G., Rood, H. J., & Thompson, L. A. 1980, *ApJ*, 235, 724
 Tarengi, M., Tifft, W. G., Chincarini, G., Rood, H. J. & Thompson, L. A. 1979, *ApJ*, 234, 793
 Tyson, J. A., Kochanski, G. P., & Dell'Antonio, I. P. 1998 *ApJ*, 498 L107
 Waxman, E. & Miralda-Escud e, J. 1995, *ApJ*, 451, 451
 Wegner, G., Colless, M., Saglia, R. P., McMahan, R. K., Davies, R. L., Burstein, D. & Baggley, G. 1999, *MNRAS*, 305, 259
 White, D. A., Jones, C., & Forman, W. 1997, *MNRAS*, 292, 419
 Williams, L. L. R., Navarro, J. F., & Bartelmann, M. 1999, *ApJ*, 527, 535
 Zabludoff, A. I., Geller, M. J., Huchra, J. P., & Ramella, M. 1993, *AJ*, 106, 1301

TABLE 1
SUMMARY OF MEASUREMENTS

Object	quantity	value	\pm
Arclet	$m_R^{(a)}$	18.55	0.03
G3	$m_R^{(a)}$	19.24	0.05
Arclet	FWHM ^(b)	0''.42	0''.08
BCG	$\epsilon_\ell^{(c)}$	0.10	0.01
SRG	$\epsilon_\ell^{(c)}$	0.33	0.02
BCG	PA ^(d)	10° 7	0° 7
SRG	PA ^(d)	161° 4	2° 0
Arclet	$c_z^{(e)}$	42665	40
BCG	$c_z^{(e)}$	13188	25
SRG	$c_z^{(e)}$	13519	25
G3	$c_z^{(e)}$	39738	25
BCG	$v_m^{(f)}$	49	5
SRG	$v_m^{(f)}$	117	7
BCG	$\sigma_0^{(g)}$	295	7
SRG	$\sigma_0^{(g)}$	271	8

^(a) R magnitude, corrected for Galactic extinction

^(b) seeing-corrected FWHM along the minor axis of arclet

^(c) ellipticity of the light distribution, at $r = 10''$

^(d) angle of major axis, east from north, at $r = 10''$

^(e) heliocentric redshift (km s^{-1})

^(f) rotational velocity (km s^{-1}) at $r \gtrsim 5''$ and $\text{PA} = 122^\circ$

^(g) central velocity dispersion (km s^{-1})

fig1.gif

FIG. 1.— An A2152 finding chart. The image was taken with Keck/LRIS through an R filter. The field is $5'.6 \times 6'.0$ in size, and the bright galaxy at center is the A2152 BCG. Several other galaxies are labeled: the second-ranked cluster galaxy (SRG); the arclet at $z = 0.142$ (A); three early-type galaxies all at $z \approx 0.133$ (G1, G2, G3); and the only other galaxy in this field with a known redshift (M). The redshifts of the BCG, SRG, and galaxy “M” are all $z \approx 0.044$. For reference, the arclet is $25''$ from the center of the BCG, and the BCG/SRG pair are separated by $47''$. The large “X” near the bright pair of background galaxies G1/G2 marks the location of the centroid of the X-ray emission, normally attributed to A2152 (Jones & Forman 1999).

This figure "fig1.gif" is available in "gif" format from:

<http://arxiv.org/ps/astro-ph/0010187v1>